

Realization of numerical aperture 2.0 using a gallium phosphide solid immersion lens

Qiang Wu,^{a)} G. D. Feke, and Robert D. Grober
Department of Applied Physics, Yale University, New Haven, Connecticut 06520

L. P. Ghislain
Digital Instruments Inc., Santa Barbara, California 93117

(Received 7 September 1999; accepted for publication 2 November 1999)

We report a study of a gallium phosphide, hemispherical, solid immersion lens through the imaging of 40-nm-diam fluorescent dye balls. A spatial resolution as small as 139 nm has been achieved at a wavelength of 560 nm, which is equivalent to a diffraction-limited system of numerical aperture 2.0. This resolution is a 33% improvement over conventional oil immersion objectives and previously reported solid immersion lenses, which typically have a numerical aperture around 1.5.
 © 1999 American Institute of Physics. [S0003-6951(99)02752-7]

Solid immersion microscopy, a technique similar to oil immersion microscopy, extends the diffraction limit by filling the object space with a high-refractive-index material. Oils used for this purpose typically have a refractive index n equal to 1.5, yielding a practical numerical aperture (NA) of order 1.4.¹ The refractive index in solids can be much larger, as large as $n \sim 3.4$ for gallium phosphide (GaP) at visible wavelengths. Previous papers report the fabrication of solid immersion lenses (SILs) from high-index glasses ($n \sim 2$),²⁻⁸ gallium phosphide,⁹ and sapphire ($n \sim 1.76$),¹⁰ the best result achieving a NA of about 1.5.^{2,5,10} It has since found application in data storage,^{3,9} lithography,⁵ and the study of semiconductor nanostructures.^{6-8,10} In this letter, we demonstrate the implementation of a hemispherical, gallium phosphide, SIL achieving an effective numerical aperture of 2.0.

The solid immersion lens was initially developed² as a technique for enhancing the spatial resolution of conventional imaging microscopy. Two types of SILs are used. One is a simple hemisphere² and the other is a standard Weierstrass optic³ in which the height of the truncated sphere is equal to $(1 + 1/n)r$, where r is the radius of curvature. It is theoretically possible for both types of SILs to perform imaging near the center of their bottom surface without geometric aberration.^{1,2,11} The advantage of the Weierstrass optic is that it has the potential to improve the NA of a far-field objective by a factor of n^2 , as compared to an improvement of a factor n for a hemispherical SIL. In both cases, the maximum achievable NA is equal to n . The disadvantage of the Weierstrass SIL is that dispersion makes it subject to severe chromatic aberration because its dimensions are dependent on n . For most materials, this aberration limits the usable bandwidth to only a few percent of the visible spectrum. A hemisphere, however, suffers only mild lateral chromatic aberration, due to the fact that the magnification of a hemisphere² n is wavelength dependent. Because the magnitude of this effect is only a few percent across the visible spectrum, the hemispherical SILs may be considered achromatic. Another advantage of the hemispherical SILs is that it

is more tolerant than the Weierstrass SIL to the thickness of the optic.¹²

The experimental setup is composed of a Zeiss Axioskop 50 microscope and a 0.8 NA Leitz-Wetzlar microscope objective with 2 mm working distance, a laser filter, a negative achromatic lens, and a TE cooled charge-coupled device (CCD) camera as shown in Fig. 1. The purpose of using a negative lens is to increase magnification to enable more accurate spot size measurements. A 500- μm -radius, grade 10, hemispherical (accurate to less than 2 μm), gallium phosphide (GaP) SIL (Ref. 13) is mounted in a conic adapter, which holds it directly on top of a slide carrying 40-nm-diam. fluorescent, polystyrene balls from Molecular Probes¹⁴ with slight contact pressure. Before each measurement, the aberration-free field of view ($\sim 10 \mu\text{m}$) (Refs. 2 and 11) is centered to the optical axis of the Leitz objective, which is

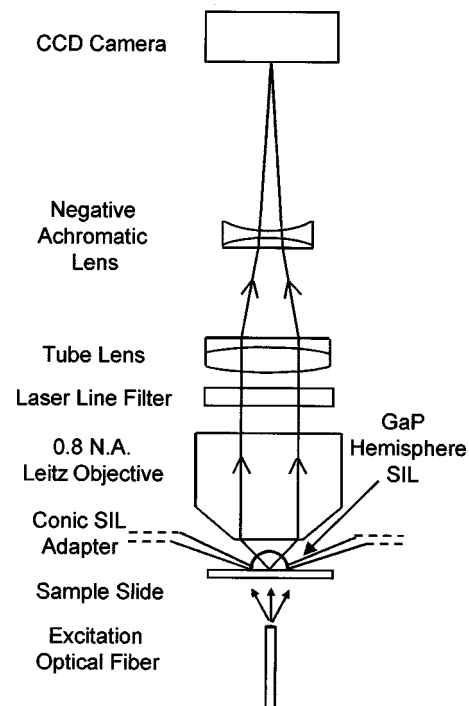


FIG. 1. Schematic of our experimental setup.

^{a)}Electronic mail: qiang.wu@yale.edu

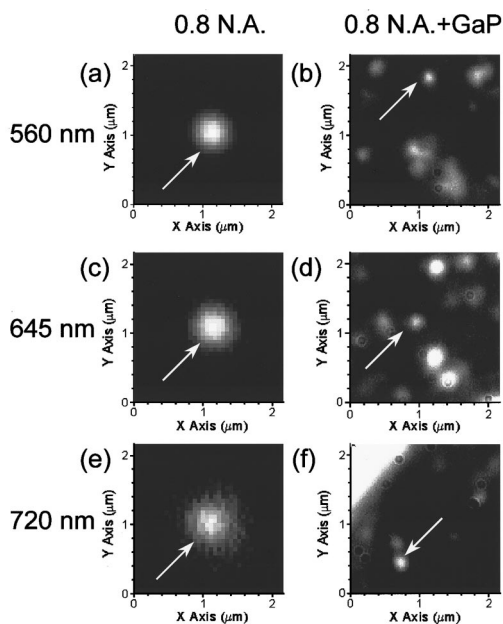


FIG. 2. (a), (c), and (e) show three images, obtained by the 0.8 NA far-field objective of dye balls with emission wavelengths of 560, 645, and 720 nm, respectively. (b), (d), and (f) show similar images obtained by the 0.8 NA objective and a hemispherical GaP SIL from different fields of view.

done by moving the SIL and the sample together using the Zeiss X–Y positioning stage. The 488 nm line of an argon ion laser is used for excitation. The fluorescence from the dye balls is imaged onto and recorded by the CCD detector. The magnification of the system is calibrated using a 3- μ m-period calibration grating.

There are two criteria commonly used in defining the spatial resolution of an optical system: Rayleigh's criterion and Sparrow's criterion.¹⁵ Rayleigh's criterion defines the resolution by measuring the distance from the center to the first zero position of a diffraction-limited spot while Sparrow's criterion defines the resolution by measuring the full width at half maximum (FWHM) of a diffraction-limited spot. Since the FWHM measurement is easier to perform and has higher accuracy, all measurements shown in this letter reference Sparrow's criterion, which defines the FWHM of a diffraction-limited spot as

$$\Delta x(\text{FWHM}) = \frac{0.51\lambda}{\text{NA}}, \quad (1)$$

where λ is the emission wavelength of the sample. This formula describes perfect imaging systems. We also use this formula to describe nearly perfect imaging systems by measuring the FWHM experimentally and using Eq. (1) to calculate an effective NA for the imaging system. We use this effective NA as a measure of the resolution of the imaging system.

To test the imaging properties of the SIL, we image the fluorescence from these 40-nm-diam fluorescent dye balls. The advantage of this experiment is that the 40-nm-diam balls approximate point sources. Images obtained both with and without the SIL are displayed in Fig. 2. Shown in Figs. 2(a), 2(c), and 2(e) are three far-field images taken from dye balls with emission wavelengths centered at 560, 645, and 720 nm, respectively. The size of the dye balls measured in

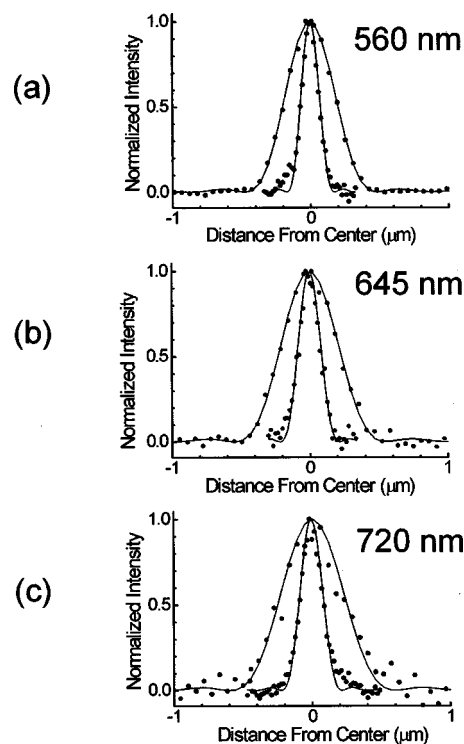


FIG. 3. Line cuts (normalized) from both the far-field and solid immersion image spots indicated by arrows in Figs. 2(a) and 2(b), 2(c) and 2(d), and 2(e) and 2(f) are shown in (a), (b), and (c), respectively.

these images is limited by the resolution of the imaging system. Images taken with the GaP SIL from different fields of view are shown in Figs. 2(b), 2(d), and 2(f). The pixel size of each of these SIL images is scaled by the index of refraction of the SIL (Ref. 16) to account for the magnification provided by the SIL. The index of refraction of GaP is known to be 3.4203, 3.2965, and 3.2401 for wavelengths 560, 645, and 720 nm, respectively.¹⁷ According to our calibration, 1 μ m equals 17.7 pixels for the three far-field images shown in Figs. 2(a), 2(c), and 2(e). For the three SIL images shown in Figs. 2(b), 2(d), and 2(f), 1 μ m equals 60.5, 58.3, and 57.3 pixels, respectively.

The fact that the dye balls appear much smaller in the SIL images clearly demonstrates that we have achieved a much higher spatial resolution with the GaP SIL. Also, in each of these three images, the size of these dye balls seems to vary. This is because the dye balls tend to aggregate, forming larger clusters. We, therefore, use the size of the smallest "dot" observed in each image as a measure of the spatial resolution of the SIL. Each such dot is indicated by an arrow in Figs. 2(a)–2(f).

To measure resolution, we take a line cut across the x axis of each dot. These are shown in Fig. 3. In each of the three plots, the broader peak is the line cut from the far-field image and the narrower one from the SIL image. A least-square fit to Airy line shape is performed for each curve, from which the FWHM value is measured. The resolution of the imaging system without the SIL, as tabulated in Table I, is determined to be between 0.72 and 0.74 NA. The fact that these values are slightly lower than the nominal NA of 0.8 specified for the objective may be due to the use of the negative achromatic lens.

The results of experiments using the SIL are also sum-

TABLE I. Calculated and measured resolutions for our far-field system both without and with the GaP solid immersion lens.

	Measured FWHM (no SIL)	Effective NA (no SIL)	Measured FWHM (with SIL)	Effective NA (with SIL)	Theoretical NA (0.73 <i>n</i>)
560 nm	397 ± 10 nm	0.72 ± 0.02	139 ± 4 nm	2.05 ± 0.05	2.50
645 nm	457 ± 11 nm	0.72 ± 0.02	175 ± 4 nm	1.88 ± 0.05	2.41
720 nm	499 ± 12 nm	0.74 ± 0.02	178 ± 5 nm	2.06 ± 0.05	2.37

marized in Table I. The experimentally measured FWHM values are 145, 180, and 183 nm for wavelengths 560, 645, and 720 nm, respectively. Since we know that we are imaging 40-nm-diam balls, it is appropriate to deconvolve their finite size from the measurements. To this end, we approximate the broadening as a simple sum of squares, $\Delta x_{\text{observed}}^2 = \Delta x_{\text{system}}^2 + \Delta x_{\text{dye ball}}^2$. This deconvolution is exact for Gaussian line shapes and should be a reasonable approximation for our purposes. The resulting FWHM for the system response is 139, 175, and 178 nm. As tabulated in Table I, these results correspond to effective numerical apertures equal to 2.05, 1.88, and 2.06, respectively, for the three wavelengths. We compare these experimental results with our theoretical expectations. We have demonstrated experimentally that our far-field system functions as 0.73 NA. Multiplying this by the index of refraction of GaP, we expect the theoretical limit of our system to be 2.50, 2.41, and 2.37 NA for the wavelengths 560, 645, and 720 nm, respectively. Note that we are within 20% of the theoretical limit for our imaging system.

Degradation in the performance of the SIL may be a result of the gap between the bottom surface of the SIL and the dye balls. Although our experiments have been carried out under clean laboratory conditions, i.e., we have carefully removed dust particles following laser optics cleaning procedures, an air gap exists because the 40 nm diam of the individual dye balls puts the center of mass at least 20 nm below the bottom surface of the SIL. In addition, the clusters clearly observed in the images likely act as spacers keeping the individual dye balls even further from the bottom surface of the SIL. A recent calculation by Baba *et al.*,¹¹ suggests that the sample has to be within $\lambda/10$ of the bottom of the SIL in order to achieve an effective NA of more than 2.0. Accordingly, our observed effective NA of 2.0 is consistent with the dye balls being approximately 60 nm below the bottom surface of the SIL.

Another factor which could limit the performance of the SIL is sphericity. Our GaP SIL is specified as grade 10 (i.e., better than 10 μm peak-to-valley sphericity), which is equivalent to a maximum absolute wave-front error $|\Delta\Phi_{\text{max}}| \cong 300 \text{ nm}$ in air. This error is equal to 0.54λ , 0.45λ , and 0.4λ for 560, 645, and 720 nm light, respectively, which is relatively large in comparison to Rayleigh's quarter wavelength rule¹ for aberration due to sphericity. Improving the sphericity of the SIL is a possible direction for future work.

We have clearly demonstrated that a SIL can be used to realize 2.0 NA, extending the lateral spatial resolution of the traditional diffraction limit by a factor of 2 while preserving much of the simplicities of far-field imaging. This result is significantly better than the resolution achievable with oil

immersion microscopy and all previously reported SIL experiments. As shown above, there is still room for improvement. It is interesting to speculate as to the upper limits of a SIL-based system. For a far-field system with 0.90 NA operating at 560 nm and using a GaP SIL, one should theoretically be able to achieve spatial resolution of order 100 nm.

In summary, we have measured the spatial resolution of a gallium phosphide, hemispherical, solid immersion lens and achieved an effective numerical aperture of 2.0 and spatial resolution as small as 139 nm using 560 nm wavelength light. We conclude that the effective numerical aperture achieved using this GaP SIL is 33% better than that of oil immersion objectives and previously reported solid immersion lenses.

The authors thank Professor Gordon S. Kino of Stanford University for very helpful discussions. This work is supported in part by the David and Lucile Packard Foundation and SRC Grant No. 98-LJ-438.

¹M. Born and E. Wolf, *Principles of Optics* (Pergamon, New York, 1980), pp. 253 and 468.

²S. M. Mansfield and G. S. Kino, *Appl. Phys. Lett.* **57**, 2615 (1990); S. M. Mansfield, Ph.D. dissertation, Stanford University, 1992.

³B. D. Terris, H. J. Mamin, D. Rugar, W. R. Studenmund, and G. S. Kino, *Appl. Phys. Lett.* **65**, 388 (1994); B. D. Terris, H. J. Mamin, and D. Rugar, *ibid.* **68**, 141 (1996).

⁴J. A. H. Stotz and M. R. Freeman, *Rev. Sci. Instrum.* **68**, 4468 (1997).

⁵L. P. Ghislain and V. B. Elings, *Appl. Phys. Lett.* **72**, 2779 (1998); L. P. Ghislain, V. B. Elings, K. B. Crozier, S. R. Manalis, S. C. Minne, K. Wilder, G. S. Kino, and C. F. Quate, *ibid.* **74**, 501 (1999).

⁶M. Yoshita, T. Sasaki, M. Baba, and H. Akiyama, *Appl. Phys. Lett.* **73**, 635 (1998); M. Yoshita, M. Baba, S. Koshihara, H. Sasaki, and H. Akiyama, *ibid.* **73**, 2965 (1998).

⁷C. D. Poweleit, A. Gunther, S. Goodnick, and J. Menendez, *Appl. Phys. Lett.* **73**, 2275 (1998).

⁸A. Chekanov, M. Birukawa, Y. Itoh, and T. Suzuki, *J. Appl. Phys.* **85**, 5324 (1999).

⁹M. Vollmer, H. Giessen, W. Stolz, W. W. Ruehle, L. P. Ghislain, and V. B. Elings, *Appl. Phys. Lett.* **74**, 1791 (1999).

¹⁰Q. Wu, R. D. Grober, D. Gammon, and D. S. Katzer, *Phys. Rev. Lett.* **83**, 2652 (1999).

¹¹M. Baba, T. Sasaki, M. Yoshita, and H. Akiyama, *J. Appl. Phys.* **85**, 6923 (1999).

¹²G. S. Kino, *Proc. SPIE* **3609**, 56 (1999).

¹³Commercially available from Digital Instruments, Santa Barbara, CA.

¹⁴TransFluoSpheres Fluorescent Microspheres, Molecular Probes Product Information Sheet No. MP 07186 (1998).

¹⁵T. R. Corle and G. S. Kino, *Confocal Scanning Microscopy and Related Imaging Systems* (Academic, New York, 1996).

¹⁶We have calibrated the system at 546 nm using a calibration grating and found that the magnification of our SIL is within 1% of the theoretical value. We, therefore, use the known refractive index to calibrate the length scale in each SIL image at its respective wavelength.

¹⁷A. Borghesi and G. Guizzetti, in *Handbook of Optical Constants of Solids*, edited by E. D. Palik (Academic, New York, 1985), p. 445.